



SHORT COMMUNICATION

Fibromodulin Is Essential for Fetal-Type Scarless Cutaneous Wound Healing



Zhong Zheng,^{*†} Xinli Zhang,^{*‡} Catherine Dang,[‡] Steven Beanes,[§] Grace X. Chang,[¶] Yao Chen,^{*} Chen-Shuang Li,^{*} Kevin S. Lee,^{*} Kang Ting,^{*†||} and Chia Soo[†]

From the Dental and Craniofacial Research Institute and Section of Orthodontics,^{*} School of Dentistry, the UCLA Division of Plastic and Reconstructive Surgery, the Department of Orthopaedic Surgery, and the Orthopaedic Hospital Research Center,[†] the Department of Surgery,[¶] David Geffen School of Medicine, and the Department of Bioengineering,^{||} School of Engineering, University of California, Los Angeles, Los Angeles; the Saul & Joyce Brandman Breast Center,[‡] Department of Surgery, Cedars-Sinai Medical Center, Los Angeles; and Hoag Hospital,[§] Newport Beach, California

Accepted for publication
July 22, 2016.

Address correspondence to
Kang Ting, D.M.D.,
D.Med.Sc., Box 951668,
30-113 CHS, Los Angeles, CA
90095-1668; or Chia Soo,
M.D., MRL 2641A, Box
951759, 675 Charles E. Young
Dr., South Los Angeles, CA
90095-1759. E-mail: [kting@
dentistry.ucla.edu](mailto:kting@dentistry.ucla.edu) or [bsoo@
ucla.edu](mailto:bsoo@ucla.edu).

In contrast to adult and late-gestation fetal skin wounds, which heal with scar, early-gestation fetal skin wounds display a remarkable capacity to heal scarlessly. Although the underlying mechanism of this transition from fetal-type scarless healing to adult-type healing with scar has been actively investigated for decades, *in utero* restoration of scarless healing in late-gestation fetal wounds has not been reported. In this study, using loss- and gain-of-function rodent fetal wound models, we identified that fibromodulin (Fm) is essential for fetal-type scarless wound healing. In particular, we found that loss of Fm can eliminate the ability of early-gestation fetal rodents to heal without scar. Meanwhile, administration of fibromodulin protein (FM) alone was capable of restoring scarless healing in late-gestation rat fetal wounds, which naturally heal with scar, as characterized by dermal appendage restoration and organized collagen architectures that were virtually indistinguishable from those in age-matched unwounded skin. High Fm levels correlated with decreased transforming growth factor (TGF)- β 1 expression and scarless repair, while low Fm levels correlated with increased TGF- β 1 expression and scar formation. This study represents the first successful *in utero* attempt to induce scarless repair in late-gestation fetal wounds by using a single protein, Fm, and highlights the crucial role that the FM-TGF- β 1 nexus plays in fetal-type scarless skin repair. (*Am J Pathol* 2016, 186: 2824–2832; <http://dx.doi.org/10.1016/j.ajpath.2016.07.023>)

Cutaneous fibrosis (scarring) affects up to 100 million patients each year.¹ It is characterized by disorganized extracellular matrix and lack of normal dermal appendages such as hair follicles.² Interestingly, skin transplantation or grafting methodologies have shown that fetal skin itself, rather than the intrauterine environment, possesses the intrinsic cells and molecular signals to heal scarlessly, with restoration of normal dermal extracellular matrix architecture and appendages.^{3–5} For example, 15- to 22-week human fetal skin grafted s.c. into athymic nude mice retained the ability to heal without scar, while this ability for scarless skin repair was lost with increasing gestational age.^{3,5} Significant research efforts have demonstrated that fetal wounds express less profibrotic factors such as transforming growth factor (TGF)- β 1, and more antifibrotic factors such as TGF- β 3^{3,6} and IL-10^{7,8} as well as a higher

This study was supported by the Plastic Surgery Foundation 2013 National Endowment for Plastic Surgery 269698; NIH-National Institute of Arthritis and Musculoskeletal and Skin Diseases grants R43AR064126, R44AR064126, and R43AR063558; and NIH-National Institute of Dental and Craniofacial Research grant R44DE024692. Confocal laser scanning microscopy was performed at the Advanced Light Microscopy/Spectroscopy Shared Resource Facility, Center for NanoScience Institute, University of California, Los Angeles (Los Angeles, CA), which was supported by NIH-National Center for Research Resources shared resources grant CJK1-443835-WS-29646 and National Science Foundation Major Research Instrumentation grant CHE-0722519.

Disclosures: Z.Z., K.T., and C.S. are inventors on fibromodulin-related patents assigned to the University of California, Los Angeles (Los Angeles, CA). Z.Z., K.T., and C.S. are founders of Scarless Laboratories Inc. (Beverly Hills, CA), which sublicenses fibromodulin-related patents from the UC Regents, who also hold equity in the company. C.S. has 79.98% shares, Z.Z. has 4.94% shares, the University of California, Los Angeles has 2.15% shares. Z.Z. and C.S. are also officers of Scarless Laboratories, Inc.

ratio of type III to type I collagen.^{3,9} However, Phase 3 human clinical trials with recombinant human TGF- β 3 (avotermin; Juvista, Renovo, Manchester, UK)¹⁰ and three Phase 2 studies with IL-10 failed to show efficacy in scar reduction.^{11,12}

In an effort to better identify key factors in scarless fetal-type repair, we used a fetal rat skin model that transitions from fetal-type scarless healing to adult-type repair with scar between embryonic days 16.5 (E16; early gestation) and 18.5 (E18; late gestation) (term, 21.5 days).^{3,9} We previously reported a significant decrease of fibromodulin (Fm) expression associated with the transition from scarless fetal-type to adult-type repair with scar.¹³ Fibromodulin protein (FM) is a small leucine-rich proteoglycan involved in angiogenesis and fibrillogenesis,^{14–18} but its role in fetal and adult cutaneous repair is not fully understood. Our current study used Fm loss- and gain-of-function wound models to determine the necessity and sufficiency of FM in fetal scarless healing.

Materials and Methods

Animal Surgery Procedures

All animal surgeries were performed under the institutionally approved protocols provided by the Chancellor's Animal Research Committee at the University of California, Los Angeles (Los Angeles, CA; protocol number 2000-058).

E16 Fetal Rat Model

Three-month-old male and female Sprague-Dawley rats were purchased from Charles River Laboratories, Inc. (Wilmington, MA), and housed in a light- and temperature-controlled animal facility at UCLA. Pregnant rats carrying fetuses at E16 were anesthetized. Using aseptic technique, laparotomy was performed via a midline incision to expose the uterus. A 7-0 Nylon purse-string suture was then placed in the uterine wall. The myometrium and amniotic sac were incised at the center of the purse string to expose the fetus as previously described.¹³ Using a microinjector (Hamilton Co., Reno, NV), 10 μ L of sterile phosphate-buffered saline (PBS) solution consisting of permanent dye and 8 mg/mL rabbit anti-FM antibody¹⁹ was injected into the fetus to raise a skin wheal. A 2-mm-diameter, circular, full-thickness skin excisional wound was generated at the site of injection. The wound was then marked with additional permanent dye, and the hysterotomy was closed by tightening of the purse-string suture. Two control groups received 10 μ L of 20 mg/mL rabbit immunoglobulin (Santa Cruz Biotechnology, Santa Cruz, CA) in PBS, or 10 μ L of PBS alone. Sterile normal saline was injected into the amniotic sac to replace lost amniotic fluid before hysterotomy closure. In a typical litter of 12 fetuses, 6 littermates were wounded, and the remaining fetuses were left unwounded. Operations were performed in 10 maternal rats. On completion of the fetal surgeries, the maternal rat was given an i.p. normal saline

fluid bolus (30 mL/kg), and the laparotomy incision was closed. Maternal rats were monitored closely for 6 hours after surgery and given food and water *ad libitum* once they had recovered from anesthesia.¹³

E18 Fetal Rat Model

Using the same technique, operations were performed on pregnant rats carrying E18 fetuses. On exposure of the fetus, 10 μ L of 0.1 mg/mL sterile recombinant human FM²⁰ in 1 mg/mL Vitrogen (type I collagen, aka PureCol; Advanced BioMatrix, San Diego, CA; to keep FM localization) was injected superficially into the dorsum of the fetus to raise a skin wheal. After the injection, a 2-mm-diameter, circular, full-thickness skin excisional wound was generated. The wounds were then marked with permanent dye, and 10 μ L of a half-strength Fm solution was applied topically to the wound. Two control groups received 10 μ L of 1 mg/mL Vitrogen, or 10 μ L PBS alone. Operations were performed in a total of 13 maternal rats.

E16 Fetal Mouse Model

Using the same hysterotomy technique described for fetal rat surgery, operations were performed on pregnant maternal 129/sv wild-type and Fm-null (*Fmod*^{-/-}) mice²¹ carrying E16 fetuses (term, 20 to 21 days). A 1-mm-diameter, circular, full-thickness skin excisional wound was generated on the dorsum of only one fetus of each litter, and the remaining littermates were left unwounded. The wounds were then marked with permanent dye. For rescue experiments, 10 μ L of recombinant human FM (0.1 mg/mL) in Vitrogen (1 mg/mL) was applied topically to the wound. A separate group treated with Vitrogen alone was used as control. Operations were performed in 12 mice per group.

Microarray Analysis

Unwounded E16 and E18 fetal rat skin samples were sent to Miltenyi Biotec GmbH (Cologne, Germany) for microarray analysis. Briefly, four E16 and three E18 total RNA samples were pooled. A total of 1 μ g of each RNA sample was amplified and labeled using the Agilent Low RNA Input Linear Amp Kit (Agilent Technologies, Santa Clara, CA) following the manufacturer's protocol. Then, the hybridization procedure was performed according to the 60-mer oligo microarray processing protocol using the Gene Expression Hybridization Kit (Agilent Technologies). A volume of 825 ng of the corresponding cyanine 3- and cyanine 5-labeled fragmented cRNA was combined and hybridized overnight (17 hours, 65°C) to Whole Rat Genome Oligo Microarray Kit, 4 \times 44K (Agilent Technologies) using the manufacturer's recommended hybridization chamber and oven. Fluorescence signals of the hybridized microarrays were detected using a DNA microarray scanner (Agilent Technologies). The Feature Extraction software package version 9.5.1.1 (Agilent Technologies) was used to read and process the microarray

image files. For the determination of differential gene expression, Feature Extraction software—derived output data files were further analyzed using the Rosetta Resolver gene expression data analysis system version 6.0 (Rosetta Biosoftware, Seattle, WA). The microarray data were submitted to Gene Expression Omnibus (<http://www.ncbi.nlm.nih.gov/geo>; accession number GSE74976).

Histologic Examination and Immunohistochemical Analysis

Animals were sacrificed at 72 hours after injury for sample harvesting. After fixation in 4% paraformaldehyde at 4°C overnight, samples were dehydrated, paraffin-embedded, and sectioned at 5- μ m increments for hematoxylin and eosin staining, or at 10- μ m increments for Picrosirius red staining. To ensure that the histologic sections were confined to the wound and not the nearby skin, the samples were sectioned with the index of the permanent dye. Immunohistochemical staining was performed and analyzed as previously described.²⁰ Primary antibody against TGF- β 1 was purchased from Santa Cruz Biotechnology. Computerized immunolocalization intensity analyses were performed using Image-Pro Plus software version 6.0 (Media Cybernetics Inc., Rockville, MD). Relative dermal protein expression was quantified as the Mean optical density of staining signal \times Percentage of area positively stained \times 100.^{20,22,23}

Confocal Laser Scanning Microscopy

After Picrosirius red staining, the dermal collagen deposition pattern of the upper dermis was evaluated by confocal microscopy on a Carl Zeiss LSM 510 META Laser scanning confocal microscope (Carl Zeiss, Oberkochen, Germany) by previously published methods.¹⁷ Since fractal dimension (F_D) and lacunarity (L) analyses are more sensitive than are conventional methods such as polarized light microscopy, X-ray diffraction, laser scattering, and Fourier transform analysis, collagen organization architecture was assessed by F_D and L analyses to quantify collagen organizational architecture in scar area as described previously.¹⁷

Real-Time Quantitative RT-PCR

Total RNA of unwounded E16 and E18 fetal rat skin was isolated using the RNeasy Mini Kit with DNase treatment (Qiagen, Valencia, CA), while wound tissues were collected by microdissection from tissue sections.²⁴ Total RNA was isolated using the RNeasy FFPE Kit (Qiagen). One microgram of total RNA was reverse-transcribed into cDNA in a 20- μ L reaction mixture with 50 pmol of oligo(dT)₂₀ primer and 1 μ L (200 U) of SuperScript III Reverse Transcriptase (Invitrogen, Foster City, CA). Expression of mRNA was measured by real-time

quantitative RT-PCR using TaqMan Gene Expression Assays on a 7500 Fast Real-Time PCR System (Applied Biosystems, Foster City, CA). Concurrent expression of glyceraldehyde-3-phosphate dehydrogenase (Gapdh) was also assessed in separate tubes for each RT reaction with TaqMan Rodent Gapdh control reagents (Applied Biosystems). Three separate sets of real-time quantitative RT-PCR analysis were performed using different complementary DNA templates.

Statistical Analysis

All statistical analyses were conducted as per consultation with the UCLA Statistical Biomathematical Consulting Clinic. Statistical analysis was performed using OriginPro software version 8 (Originlab Corp., Northampton, MA). Data are generally presented as means \pm SD. $P < 0.05$ was considered statistically significant. Two-sample t -tests were used to compare results between two groups.

Results

FM Is Necessary and Sufficient for Fetal-Type Scarless Wound Healing

Global gene profiling revealed that the expression of Fm was significantly decreased during the transition from fetal-type scarless healing to adult-type repair with scar between E16 to E18 in a fetal rat cutaneous wound model, while the expression of other small leucine-rich proteoglycans was increased or unchanged ([Supplemental Figure S1A](#) and [Supplemental Table S1](#)) and was further confirmed by real-time quantitative RT-PCR ([Supplemental Figure S1B](#)). Furthermore, in a loss-of-function experiment, injection of anti-FM antibody was sufficient to induce scar formation in normally scarless E16 rat wounds, which was not seen in PBS- and IgG-treated wounds ([Figure 1A](#)). The scarring in anti-FM antibody-treated E16 wounds resembled scarring in E18 rat wounds: Both were characterized by absent dermal appendages (eg, hair follicles) ([Figure 1B](#)) and a denser, more disorderly collagen deposition pattern ([Figure 1A](#)). To quantitate collagen organizational architecture, we performed F_D and L analyses. F_D provides a measure of how completely an object fills space, and it quantifies an object in terms of shape, regularity, lack of smoothness, size, and number of self-similarities (ie, invariance regardless of scale).²⁵ In general, a higher F_D value indicates uniform distribution.²⁵ In contrast, L permits an analysis of density, packing, or dispersion through scales. In other words, L is a measure of the heterogeneity of a structure or the degree of structural variance within an object, which is related to the distribution of empty spaces (lacunas) of an image.²⁵ Objects with lower L values are of a finer texture, while

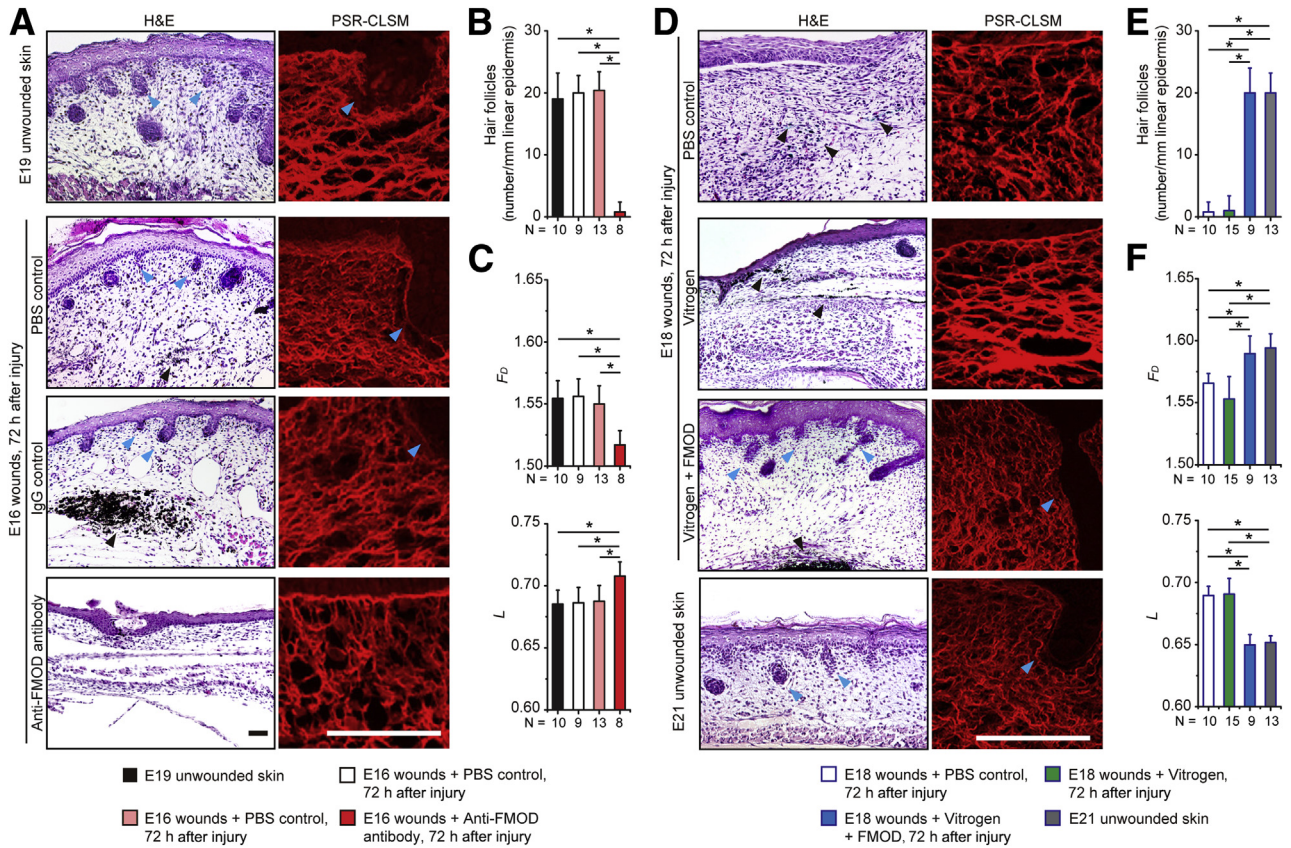


Figure 1 Fibromodulin (Fm) plays a crucial role in rat fetal-type scarless wound healing. **A:** At 72 hours after injury, phosphate-buffered saline (PBS)- and IgG-treated embryonic day 16.5 (E16) wounds heal scarlessly and are indistinguishable from age-matched unwounded embryonic day 19.5 (E19) skin. However, anti-FM antibody–treated E16 wounds heal with scar formation. **B and C:** Hair follicle densities are analyzed based on hematoxylin and eosin (H&E) staining (**B**), while fractal dimension (F_D) and lacunarity (L) are analyzed based on Picrosirius red–confocal laser scanning microscopy (PSR-CLSM) imagery (**C**). **D–F:** PBS- and Vitrogen-treated embryonic day 18.5 (E18) wounds heal with scarring at 72 hours after injury. Vitrogen + Fm–treated E18 wounds heal without scar, and the regenerated tissue resembles unwounded embryonic day 21.5 (E21) skin (**D**), accompanied by hair follicle densities analysis (**E**) and F_D and L analyses (**F**). **Blue arrowhead**, hair follicle; **black arrowhead**, surgical dye. Data are expressed as means \pm SD. $n = 8$ (**A**, anti-Fm antibody); $n = 9$ (**A**, PBS; **D–F**, Vitrogen + Fm); $n = 10$ (**C–F**, PBS); $n = 13$ (**A**, IgG); $n = 15$ (**C–F**, Vitrogen). * $P < 0.05$ (two-sample t -test). Scale bar = 100 μ m.

higher L values indicate that objects are more spatially unorganized.²⁶ In this study, we showed that anti-Fm antibody treatment decreased the mean F_D value but increased the mean L value of the E16 rat wounds in comparison with those in other groups (**Figure 1C**), indicating that the collagen fibers in those wounds were disorganized or less uniform. On the other hand, 72 hours after injury, PBS- and IgG-treated E16 rat wounds had F_D and L values similar to those of age-matched unwounded skin (**Figure 1C**). Additionally, while unwounded *Fmod*^{-/-} mice²¹ showed normal dermal histologic architecture, E16 *Fmod*^{-/-} mouse wounds healed with scarring characterized by a hypertrophic epidermis and absence of dermal appendages compared with E16 wild-type control wounds displaying normal scarless healing, which were partially rescued by application of FM protein in a Vitrogen vehicle but not by Vitrogen alone (**Figure 2**). These findings demonstrated that loss of a single extracellular matrix proteoglycan, Fm, caused normally scarless E16 fetal rodent skin wounds to heal with scar.

On the other hand, in a gain-of-function experiment, we demonstrated that the administration of FM protein in a Vitrogen collagen vehicle prevented scar formation in E18 rats; surprisingly, the wounds healed scarlessly, with hair follicles and a more organized collagen architecture that were virtually indistinguishable from those in age-matched unwounded skin (**Figure 1, D and E**). However, PBS- and Vitrogen-treated E18 wounds healed with scar as expected, accompanied by a lower mean F_D value and a higher mean L value at 72 hours after injury in comparison with unwounded E21 skin (**Figure 1, D–F**). Moreover, FM treatment increased the mean F_D value and decreased the mean L value of E18 wounds at 72 hours after injury to the same levels as these values in unwounded E21 skin (**Figure 1F**), representing more organized collagen fibers. Therefore, the addition of FM alone was sufficient to regenerate scarless fetal-type wound healing in late-gestation animals, which normally exhibit adult-type repair with scar.

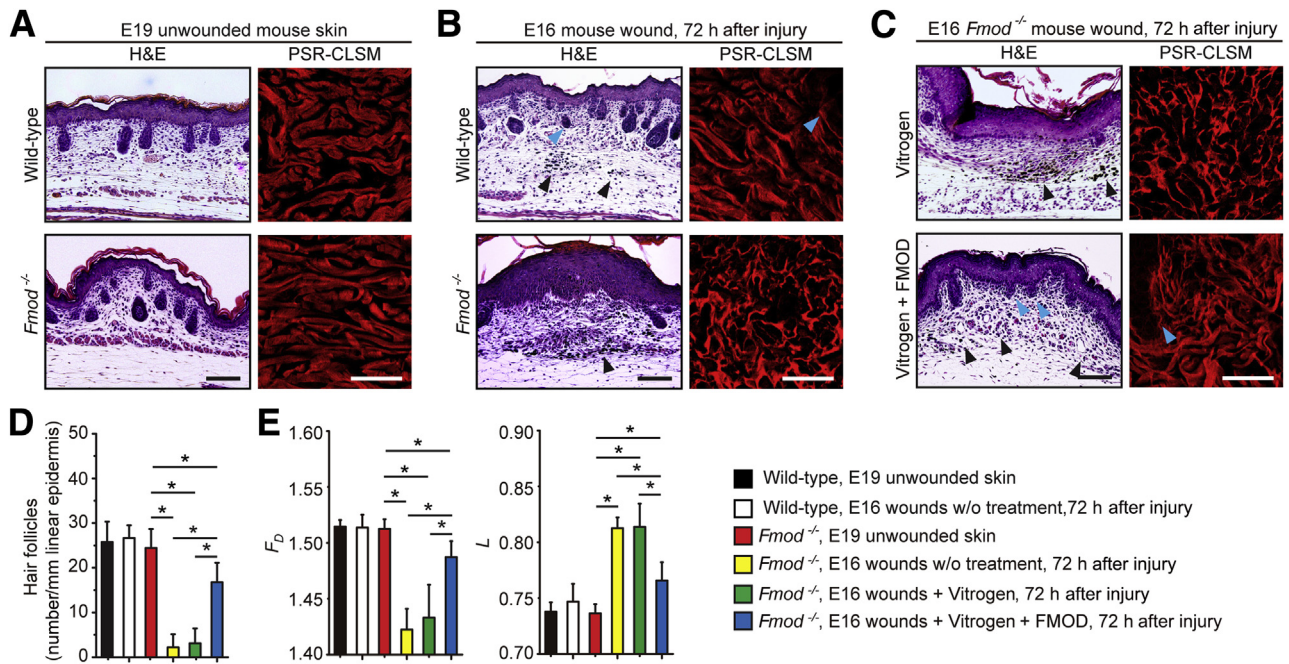


Figure 2 Fibromodulin (Fm) deficiency leads to scar formation in embryonic day 16.5 (E16) fetal mouse wounds. **A:** Unwounded embryonic day 19.5 (E19) wild-type (WT) and *Fmod*^{-/-} mouse skin shows no significant histologic difference. **B:** At 72 hours after injury, E16 fetal mouse wounds shows scarless repair, while E16 *Fmod*^{-/-} fetal mouse wounds present scar formation characterized by the absence of hair follicles and epidermal hypertrophy. **C:** Administration of FM with Vitrogen partially restores scarless wound healing in E16 *Fmod*^{-/-} wounds, while Vitrogen control alone fails to do so. Hair follicle densities are analyzed based on hematoxylin and eosin (H&E) staining (**D**), while fractal dimension (F_D) and lacunarity (L) are analyzed based on Picosirius red—confocal laser scanning microscopy (PSR-CLSM) imagery (**E**). **Blue arrowhead**, hair follicle; **black arrowhead**, surgical dye. Data are expressed as means \pm SD. $n = 6$. $*P < 0.05$ (two-sample t -test). Scale bars: 50 μ m (black); 25 μ m (white).

Taken together, these findings demonstrate that FM is both necessary and sufficient for fetal scarless repair in rodents. Importantly, FM application can reverse scarring in late-gestation fetal rodent wounds.

Fm Levels Inversely Correlate with Tgf- β 1 Levels in Fetal Rodent Wound Models

Because previous studies revealed that fetal-type scarless wounds express less Tgf- β 1 compared with adult-type scarring wounds,^{3,6} we next evaluated Tgf- β 1 expression in Fm gain- and loss-of-function fetal wound models to assess for a possible correlation. The scars formed in E18 rats treated with Vitrogen control presented strong Tgf- β 1 immunohistochemical analysis staining throughout the epidermis and dermis (**Figure 3A**). Conversely, scarless wounds in FM-treated E18 rats exhibited markedly less Tgf- β 1 staining in the epidermis and limited Tgf- β 1 staining in the dermis (**Figure 3, A and B**). Accordingly, real-time quantitative RT-PCR revealed increased Tgf- β 1 mRNA levels in collagen control-treated E18 rat wounds at 72 hours after injury compared with the Fm-treated wounds, the Tgf- β 1 expression of which was reduced to the level in unwounded skin (**Figure 3C**). Similarly, transcription of Tgf- β 1 downstream target *Col1 α 1* (encoding α_1 chain of type I collagen) was also elevated

in E18 rat wounds treated with Vitrogen control, but *Col3 α_1* (encoding α_1 chain of type III collagen) did not show an increase (**Figure 3D**). Thus, it resulted in a decreased ratio of type III to type I collagen. As expected, FM application eliminated the injury-induced increase of Tgf- β 1, and *Col1 α 1* increased in E18 rat wounds (**Figure 3, C and D**). Meanwhile, E16 *Fmod*^{-/-} mouse wounds that healed with scarring showed significantly increased Tgf- β 1 expression compared with wild-type wounds accompanied by higher *Col1 α 1* transcription. However, FM administration significantly reduced Tgf- β 1 expression in E16 *Fmod*^{-/-} wounds and promoted scarless healing (**Figure 4**). These data suggest that FM promotes fetal-type scarless cutaneous wound repair through, in part, the modulation of TGF- β 1 expression and function.

Discussion

In the current study, we demonstrated that Fm is both necessary and sufficient for fetal scarless skin repair in rodents and that FM administration significantly alters Tgf- β 1 expression. The application of FM represents the first successful attempt to use a noncytokine/growth factor, protein-based approach to restore scarless cutaneous repair in late-gestation fetal animals *in utero*.

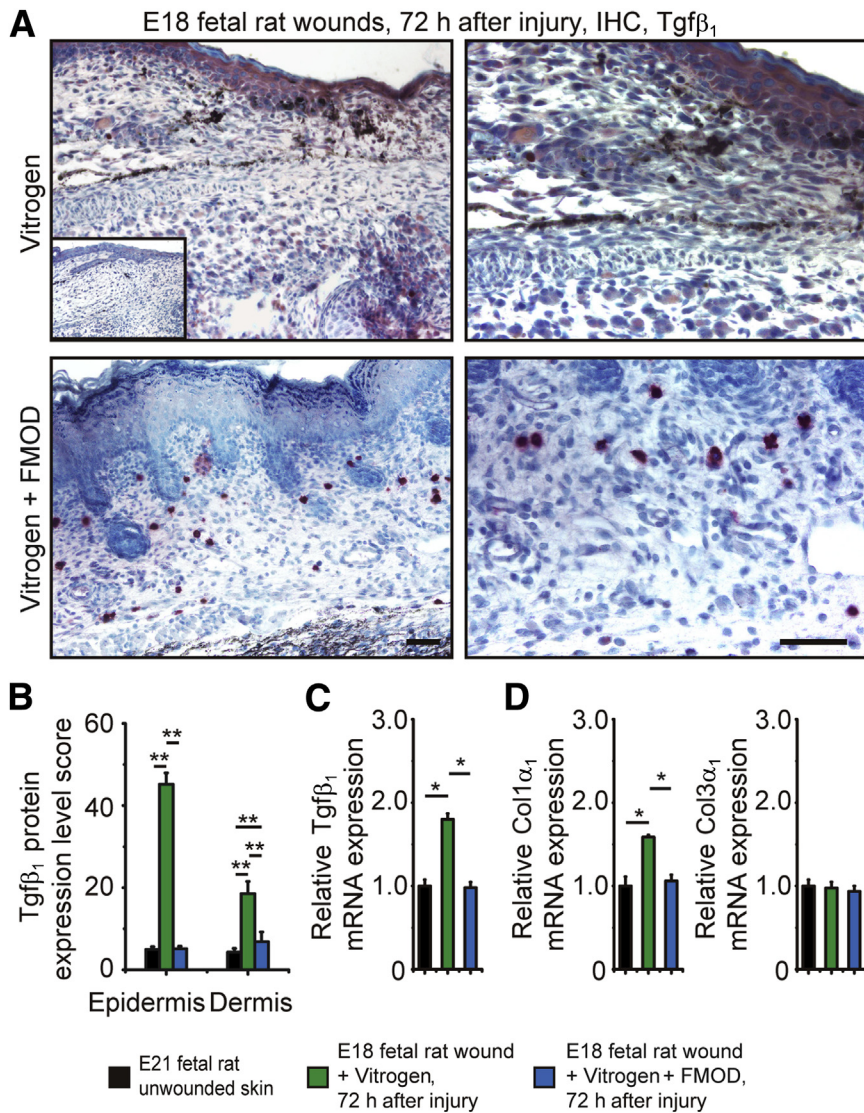


Figure 3 Fibromodulin (Fm) reduces transforming growth factor (Tgf)-β1 expression in embryonic day 18.5 (E18) fetal rat wounds. **A**: Compared with Vitrogen alone, Vitrogen + Fm significantly reduces Tgf-β1 protein expression in E18 rat wounds at 72 hours after injury [inset depicts unwounded embryonic day 21.5 (E21) rat skin]. **B** and **C**: Quantification of protein expression (**B**) and real-time quantitative RT-PCR analyses (**C**) further reveal that Vitrogen control-treated E18 rat wounds approximately double transcription of Tgf-β1 compared with unwounded E21 rat skin. However, Vitrogen + FM application markedly reduces Tgf-β1 expression to the levels of age-matched unwounded E21 rat skin. A similar transcription pattern is also observed in Col1α1 (encoding α1 chain of type I collagen) instead of Col3α1. Real-time quantitative RT-PCR data are normalized to unwounded E21 rat skin. Data are expressed as means ± SD. n = 3 pools (3 fetal wounds per pool, 9 fetuses total; **C** and **D**); n = 9 fetuses (**B**). *P < 0.05, **P < 0.01 (two-sample t-test). Scale bar = 50 μm. IHC, immunohistochemistry.

TGF-β ligands have been implicated in the ontogenetic transition from fetal-type scarless healing to adult-type repair with scar.^{3–5,13,27,28} The three mammalian TGF-β isoforms (TGF-β1, -β2, and -β3) have nonredundant and oftentimes opposing effects.^{27–30} In particular, TGF-β1 is thought to promote scar since TGF-β1 alone is enough to induce scar in wounded human fetal skin transplanted onto athymic adult mice.³¹ Moreover, neutralization of TGF-β1 reduces scar formation in adult wound models.^{32–34} Our previous studies showed that Fm deficiency markedly altered the levels and spatiotemporal expression patterns of Tgf-β ligands and receptors during wound healing.^{20,23} In addition, adenovirus-mediated FM overexpression decreased TGF-β1 expression in human dermal fibroblasts.³⁵ In this study, we observed an inverse correlation between FM and Tgf-β1 with its downstream fibrosis target, type I collagen, in fetal cutaneous wound models: High FM levels correlated with decreased Tgf-β1

expression and scarless repair, while low FM levels correlated with increased Tgf-β1 expression and scar formation. Therefore, our current finding strongly suggests that FM plays crucial regulatory roles in TGF-β signaling during cutaneous wound repair.

Interestingly, we previously also found FM to be proangiogenic^{14,15} and capable of reprogramming somatic cells to a multipotent state.^{36,37} This finding, coupled with those from our current study, support the growing consensus that FM (and other small leucine-rich proteoglycans) has pleiotropic functions regulating intracellular signaling, cell fate determination, and stem cell niches^{36–40} that extend far beyond its initially described roles in collagen assembly, organization, and degradation for extracellular matrix structural support.^{18,41–43}

In conclusion, the findings from our study suggest that FM alone is sufficient to restore scarless fetal repair to late-gestation animals, which normally heal with

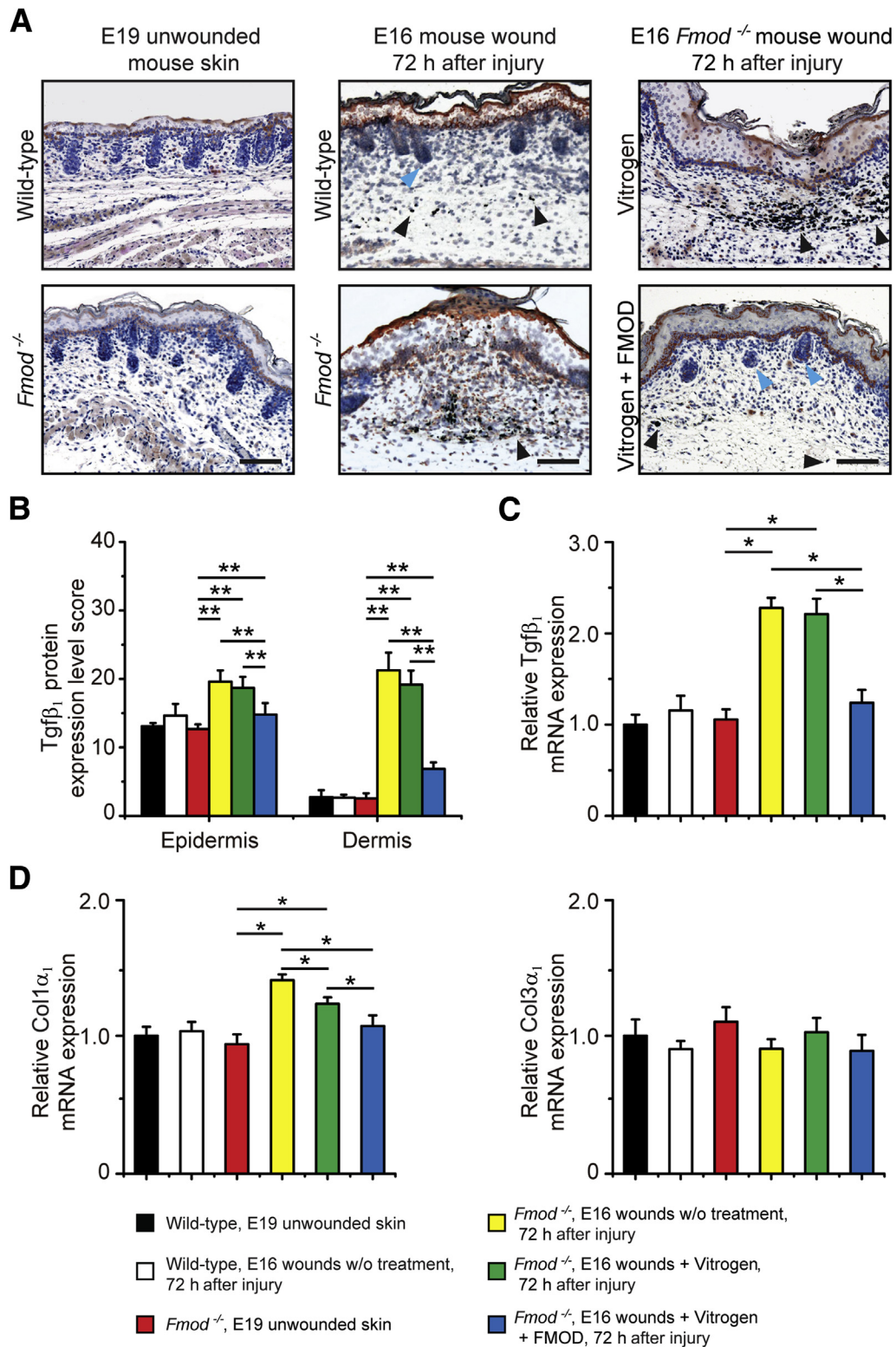


Figure 4 Fibromodulin (Fm) deficiency leads to increased transforming growth factor (Tgf-β1) expression in embryonic day 16.5 (E16) fetal mouse wounds. **A:** Compared with E16 wild-type (WT) fetal mouse wounds, E16 *Fmod*^{-/-} fetal mouse wounds exhibit increased Tgf-β1 staining at 72 hours after injury. Furthermore, the increased Tgf-β1 expression in E16 *Fmod*^{-/-} fetal wounds are not weakened by Vitrogen collagen control but are decreased by Vitrogen + FM. **B** and **C:** These phenomena are confirmed by quantification of protein expression (**B**) and real-time quantitative RT-PCR analyses (**C**). **D:** A similar transcription pattern is also observed in Col1α₁ (encoding α₁ chain of type I collagen) instead of Col3α₁. **Blue arrowhead**, hair follicle; and **black arrowhead**, surgical dye. Real-time quantitative RT-PCR data are normalized to unwounded embryonic day 19.5 (E19) mouse skin. Data are expressed as means ± SD. *n* = 3 pools (3 fetal wounds per pool, 9 fetuses total; **C** and **D**); *n* = 6 (**B**). **P* < 0.05, ***P* < 0.01 (two-sample *t*-test). Scale bar = 50 μm.

scar, and that loss of Fm alone is sufficient to induce scar in early-gestation animals, which normally heal without scar.

Acknowledgments

Fm-null animals were kindly provided by Dr. Ake Oldberg (Lund University, Lund, Sweden).

The content is solely the responsibility of the authors and does not necessarily represent the official views of the NIH.

Supplemental Data

Supplemental material for this article can be found at <http://dx.doi.org/10.1016/j.ajpath.2016.07.023>.

References

- Sund B: New Developments in Wound Care. London, PJB Publications, 2000. pp. 1–255
- Eming SA, Martin P, Tomic-Canic M: Wound repair and regeneration: mechanisms, signaling, and translation. *Sci Transl Med* 2014, 6:265sr6
- Larson BJ, Longaker MT, Lorenz HP: Scarless fetal wound healing: a basic science review. *Plast Reconstr Surg* 2010, 126:1172–1180
- Rolfe KJ, Grobbelaar AO: A review of fetal scarless healing. *ISRN Dermatol* 2012, 2012:698034
- Lo DD, Zimmermann AS, Nauta A, Longaker MT, Lorenz HP: Scarless fetal skin wound healing update. *Birth Defects Res C Embryo Today* 2012, 96:237–247
- Soo C, Beanes SR, Hu FY, Zhang X, Dang C, Chang G, Wang Y, Nishimura I, Freymiller E, Longaker MT, Lorenz HP, Ting K: Ontogenetic transition in fetal wound transforming growth factor-beta regulation correlates with collagen organization. *Am J Pathol* 2003, 163:2459–2476
- Liechty KW, Kim HB, Adzick NS, Crombleholme TM: Fetal wound repair results in scar formation in interleukin-10-deficient mice in a syngeneic murine model of scarless fetal wound repair. *J Pediatr Surg* 2000, 35:866–872; discussion 72–73
- Gordon A, Kozin ED, Keswani SG, Vaikunth SS, Katz AB, Zoltick PW, Favata M, Radu AP, Soslowsky LJ, Herlyn M, Crombleholme TM: Permissive environment in postnatal wounds induced by adenoviral-mediated overexpression of the anti-inflammatory cytokine interleukin-10 prevents scar formation. *Wound Repair Regen* 2008, 16:70–79
- Beanes SR, Hu FY, Soo C, Dang CM, Urata M, Ting K, Atkinson JB, Benhaim P, Hedrick MH, Lorenz HP: Confocal microscopic analysis of scarless repair in the fetal rat: defining the transition. *Plast Reconstr Surg* 2002, 109:160–170
- Longaker MT, Rohrich RJ, Greenberg L, Furnas H, Wald R, Bansal V, Seify H, Tran A, Weston J, Korman JM, Chan R, Kaufman D, Dev VR, Mele JA, Januszyk M, Cowley C, McLaughlin P, Beasley B, Gurtner GC: A randomized controlled trial of the Embrace advanced scar therapy device to reduce incisional scar formation. *Plast Reconstr Surg* 2014, 134:536–546
- Kieran I, Knock A, Bush J, So K, Metcalfe A, Hobson R, Mason T, O’Kane S, Ferguson M: Interleukin-10 reduces scar formation in both animal and human cutaneous wounds: results of two preclinical and phase II randomized control studies. *Wound Repair Regen* 2013, 21: 428–436
- Kieran I, Taylor C, Bush J, Rance M, So K, Boanas A, Metcalfe A, Hobson R, Goldspink N, Hutchison J, Ferguson M: Effects of interleukin-10 on cutaneous wounds and scars in humans of African continental ancestral origin. *Wound Repair Regen* 2014, 22:326–333
- Soo C, Hu FY, Zhang X, Wang Y, Beanes SR, Lorenz HP, Hedrick MH, Mackool RJ, Plaas A, Kim SJ, Longaker MT, Freymiller E, Ting K: Differential expression of fibromodulin, a transforming growth factor-beta modulator, in fetal skin development and scarless repair. *Am J Pathol* 2000, 157:423–433
- Jian J, Zheng Z, Zhang K, Rackhon TM, Hsu C, Levin A, Enjamuri DR, Zhang X, Ting K, Soo C: Fibromodulin promoted in vitro and in vivo angiogenesis. *Biochem Biophys Res Commun* 2013, 436:530–535
- Zheng Z, Jian J, Velasco O, Hsu CY, Zhang K, Levin A, Murphy M, Zhang X, Ting K, Soo C: Fibromodulin enhances angiogenesis during cutaneous wound healing. *Plast Reconstr Surg Glob Open* 2014, 2: e275
- Adini I, Ghosh K, Adini A, Chi ZL, Yoshimura T, Benny O, Connor KM, Rogers MS, Bazinet L, Birsner AE, Bielenberg DR, D’Amato RJ: Melanocyte-secreted fibromodulin promotes an angiogenic microenvironment. *J Clin Invest* 2014, 124:425–436
- Khorasani H, Zheng Z, Nguyen C, Zara J, Zhang X, Wang J, Ting K, Soo C: A quantitative approach to scar analysis. *Am J Pathol* 2011, 178:621–628
- Iozzo RV, Goldoni S, Berendsen AD, Young MF: Small leucine-rich proteoglycans. Edited by Mecham RP. In *The Extracellular Matrix: An Overview*. Berlin, Heidelberg: Springer, 2011. pp. 197–231
- Plaas AH, Wong-Palms S: Biosynthetic mechanisms for the addition of polylysine to chondrocyte fibromodulin. *J Biol Chem* 1993, 268: 26634–26644
- Zheng Z, Nguyen C, Zhang X, Khorasani H, Wang JZ, Zara JN, Chu F, Yin W, Pang S, Le A, Ting K, Soo C: Delayed wound closure in fibromodulin-deficient mice is associated with increased TGF-beta3 signaling. *J Invest Dermatol* 2011, 131:769–778
- Svensson L, Aszodi A, Reinhold F, Heinegard D, Oldberg A: Fibromodulin-null mice have abnormal collagen fibrils, tissue organization, and altered lumican deposition in tendon. *J Biol Chem* 1999, 274: 9636–9647
- Allen A, Southern S: A novel technique of computer-assisted image analysis to quantify molecular stress in cetaceans, 2002. Available at <https://swfsc.noaa.gov/publications/CR/2002/2002Allen.pdf> (accessed July 7, 2016)
- Zheng Z, Lee KS, Zhang X, Nguyen C, Hsu C, Wang JZ, Rackohn TM, Enjamuri DR, Murphy M, Ting K, Soo C: Fibromodulin-deficiency alters temporospatial expression patterns of transforming growth factor-beta ligands and receptors during adult mouse skin wound healing. *PLoS One* 2014, 9:e90817
- Erickson HS, Gillespie JW, Emmert-Buck MR: Tissue microdissection. *Methods Mol Biol* 2008, 424:433–448
- Smith TG Jr, Lange GD, Marks WB: Fractal methods and results in cellular morphology—dimensions, lacunarity and multifractals. *J Neurosci Methods* 1996, 69:123–136
- Ling EJ, Servio P, Kietzig AM: Fractal and lacunarity analyses: quantitative characterization of hierarchical surface topographies. *Microsc Microanal* 2016, 22:168–177
- Roberts AB, Sporn MB: Transforming growth factor-beta. Edited by Clark RA. In *The molecular and cellular biology of wound repair*. New York: Plenum Press, 1996. pp. 275–308
- O’Kane S, Ferguson MW: Transforming growth factor betas and wound healing. *Int J Biochem Cell Biol* 1997, 29:63–78
- Penn JW, Grobbelaar AO, Rolfe KJ: The role of the TGF-beta family in wound healing, burns and scarring: a review. *Int J Burns Trauma* 2012, 2:18–28
- Finnson KW, McLean S, Di Guglielmo GM, Philip A: Dynamics of transforming growth factor beta signaling in wound healing and scarring. *Adv Wound Care* 2013, 2:195–214
- Lin RY, Sullivan KM, Argenta PA, Meuli M, Lorenz HP, Adzick NS: Exogenous transforming growth factor-beta amplifies its own

- expression and induces scar formation in a model of human fetal skin repair. *Ann Surg* 1995, 222:146–154
32. Shah M, Foreman DM, Ferguson MW: Control of scarring in adult wounds by neutralising antibody to transforming growth factor beta. *Lancet* 1992, 339:213–214
 33. Shah M, Foreman DM, Ferguson MWJ: Neutralising antibody to TGF-beta_{1,2} reduces cutaneous scarring in adult rodents. *J Cell Sci* 1994, 107:1137–1157
 34. Shah M, Foreman DM, Ferguson MW: Neutralisation of TGF-beta 1 and TGF-beta 2 or exogenous addition of TGF-beta 3 to cutaneous rat wounds reduces scarring. *J Cell Sci* 1995, 108: 985–1002
 35. Stoff A, Rivera AA, Mathis JM, Moore ST, Banerjee NS, Everts M, Espinosa-de-los-Monteros A, Novak Z, Vasconez LO, Broker TR, Richter DF, Feldman D, Siegal GP, Stoff-Khalili MA, Curiel DT: Effect of adenoviral mediated overexpression of fibromodulin on human dermal fibroblasts and scar formation in full-thickness incisional wounds. *J Mol Med* 2007, 85:481–496
 36. Zheng Z, Jian J, Zhang X, Zara JN, Yin W, Chiang M, Liu Y, Wang J, Pang S, Ting K, Soo C: Reprogramming of human fibroblasts into multipotent cells with a single ECM proteoglycan, fibromodulin. *Biomaterials* 2012, 33:5821–5831
 37. Li CS, Yang P, Ting K, Aghaloo T, Lee S, Zhang Y, Khalilinejad K, Murphy MC, Pan HC, Zhang X, Wu B, Zhou YH, Zhao Z, Zheng Z, Soo C: Fibromodulin reprogrammed cells: a novel cell source for bone regeneration. *Biomaterials* 2016, 83:194–206
 38. Bi Y, Ehrichtou D, Kilts TM, Inkson CA, Embree MC, Sonoyama W, Li L, Leet AI, Seo BM, Zhang L, Shi S, Young MF: Identification of tendon stem/progenitor cells and the role of the extracellular matrix in their niche. *Nat Med* 2007, 13:1219–1227
 39. Popov C, Burggraf M, Kreja L, Ignatius A, Schieker M, Docheva D: Mechanical stimulation of human tendon stem/progenitor cells results in upregulation of matrix proteins, integrins and MMPs, and activation of p38 and ERK1/2 kinases. *BMC Mol Biol* 2015, 16:6
 40. Augusto LM, Aguiar DP, Bonfim DC, Dos Santos Cavalcanti A, Casado PL, Duarte ME: Mesenchymal stromal cells from bone marrow treated with bovine tendon extract acquire the phenotype of mature tenocytes. *Rev Bras Ortop* 2016, 51:70–74
 41. Merline R, Schaefer RM, Schaefer L: The matricellular functions of small leucine-rich proteoglycans (SLRPs). *J Cell Commun Signal* 2009, 3:323–335
 42. Shami A, Tengryd C, Asciutto G, Bengtsson E, Nilsson J, Hultgardh-Nilsson A, Goncalves I: Expression of fibromodulin in carotid atherosclerotic plaques is associated with diabetes and cerebrovascular events. *Atherosclerosis* 2015, 241:701–708
 43. Kurylo MP, Grandfield K, Marshall GW, Altoe V, Aloni S, Ho SP: Effect of proteoglycans at interfaces as related to location, architecture, and mechanical cues. *Arch Oral Biol* 2016, 63:82–92